Novel Bis-betaines and Betaines within [1_4]*meta*-Heterophane Frameworks**

Ermitas Alcalde,*[a] Neus Mesquida,[a] Lluïsa Pérez-García,[a] Susana Ramos,[a] Montserrat Alemany,[a] and Matías L. Rodríguez[b]

Abstract: After prior selection of betaine building blocks for the construction of quadrupolar heterophane frameworks, a convergent "3+1" synthetic strategy is reported for the synthesis of the title macrocycles composed of heterocyclic betaine subunit(s). These typify the first example of simple cyclophanes constructed out of both highly π-excessive and highly π-deficient heteroaromatic moieties linked in a 1,3-alternating fashion. The chemical reactivity of the quadrupolar heterophanes **1a** and **1c** toward electrophiles under neutral conditions corroborated their bis-betaine structure. The structural features of the bis-betaines **1**, betaines **2**$\cdot$PF$_6$ and **5**$\cdot$X, and the corresponding dicationic [1_4]heterophanes **3**$\cdot$2X and **4**$\cdot$2Cl were studied by ^{1}H and ^{13}C NMR spectroscopy and electrospray ionization mass spectrometry, and confirmed by single-crystal X-ray diffraction analysis of macrocycles **1a** and **2a**$\cdot$PF$_6$.

Keywords: betaines · cyclophanes · heterocycles · X-ray diffraction

Introduction

The molecular diversity present in macrocycles allows the design of novel molecular systems that exhibit increasingly more specific properties.[2, 3] Among them cyclophanes, phanes, and heterophanes constitute a source of a broad array of molecular architectures.[2] As a development on the chemistry of heterocyclic betaines pursued by our research group, the first systems we examined were the nonclassical [1_4]*meta*-heterophanes that contain heterocyclic betaines as building blocks, such as the quadrupolar and dipolar heterophanes **1a**, **1b**, **2a**$\cdot$PF$_6$, and **2b**$\cdot$PF$_6$, as well as their immediate precursors **3a**$\cdot$2X **and 3b**$\cdot$2X (Scheme 1), with

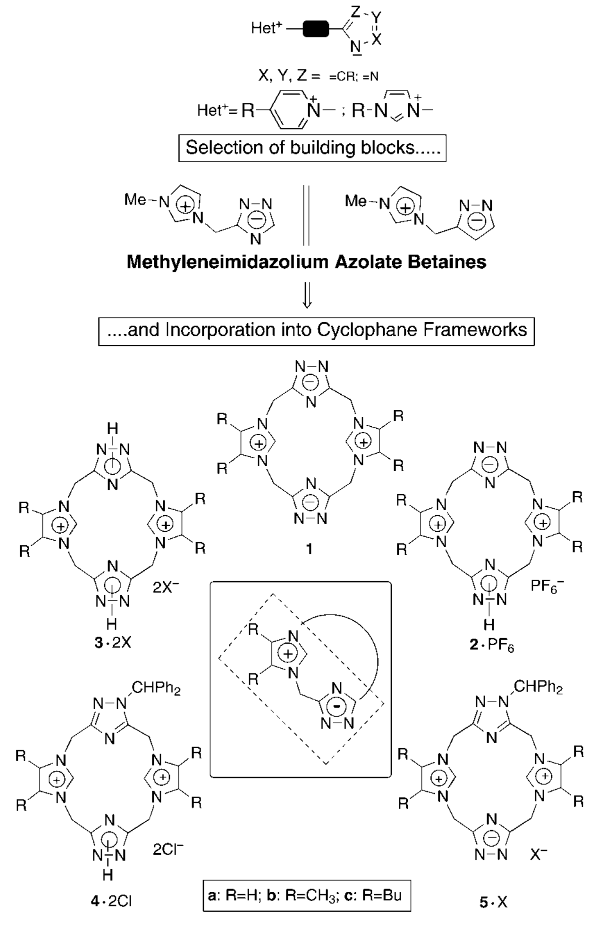

Scheme 1. Nonclassical [1_4]*meta*-heterophanes containing heterocyclic betaines as building blocks, together with their precursors.

---

[a] Prof. E. Alcalde, Dr. N. Mesquida, Dr. Ll. Pérez-García, S. Ramos, Dr. M. Alemany
Laboratori de Química Orgànica
Facultat de Farmàcia, Universitat de Barcelona
Avda. Joan XXIII s/n, 08028 Barcelona (Spain)
Fax: (+34) 93-4021896
E-mail: betaines@farmacia.far.ub.es

[b] Prof. M. L. Rodríguez
Instituto Universitario de Bio-Orgánica
Universidad de La Laguna
38206 La Laguna, Tenerife (Spain)

[**] Heterocyclic Betaines, Part 46; for Part 45 see: ref. [1].

Supporting information for this article is available on the WWW under http://wiley-vch.de/home/chemistry/ or from the author: synthesis and characterization of 3-methyl-1-imidazoliomethyl-3(5)pyrazolate; molecular structure of **1a**; unit cell packing diagram of **1a**; partial crystal packing of **1a** along the *b* axis, showing the water chain formation; molecular structure of **2a**$\cdot$PF$_6$; significant nonbonding distances for **2a**$\cdot$PF$_6$; unit cell packing diagram of **2a**$\cdot$PF$_6$; stacking mode of **2a**$\cdot$PF$_6$, showing the interplanar contacts.

0947-6539/02/0802-0474 $ 17.50+.50/0

1,3-alternating proton-ionizable 1,2,4-triazoles and quaternary imidazolium rings.[4]

The design of these supramolecular scaffolds was undertaken after careful scrutiny of several betaine building blocks—a set of methyleneazolium azolate betaines, designed by combining a variety of heterocyclic fragments based on pyrazole, 1,2,4-triazole, and benzimidazole has been described previously.[5] From these findings, as well as the results described in this work, we concluded that methyleneimidazolium-1,2,4-triazolate betaine subunits constituted the most suitable building blocks, and these were selected, mainly on the basis of their physical properties and their chemical stability, for initial studies of the construction of quadrupolar $[1_n]$heterophanes. Incorporation of methyleneimidazolium pyrazolate betaines into cyclophane frameworks might result in stable macrocyclic betaines despite the instability of the betaine subunits, as has been described for related pyridinium quadrupolar $[1_n]$heterophanes.[1]

Here we report an alternative and convenient route to the key intermediates **3a**·2X and **3b**·2X by deprotection of the *N*-benzhydryl dicationic heterophanes **4a**·2X and **4b**·2X. This synthetic pathway is the method of choice for their preparation since it both optimizes yields and allows us to obtain crystals of **1a** and **2a**·PF_6 suitable for X-ray analysis. Dications **3a**·2X, **3b**·2X, **4a**·2X, and **4b**·2X were then transformed into simple quadrupolar systems **1a** and **1b** and into the dipolar macrocycles **2a**·PF_6, **2b**·PF_6, **5a**·X, and **5b**·X, respectively. The structural properties of the betaines and bis-betaines were examined by ^1H and ^{13}C NMR spectroscopy, together with electrospray ionization mass spectrometry. Single-crystal X-ray analyses of **1a** and **2a**·PF_6 confirmed their quadrupolar and dipolar character.

The interaction of bis-betaines **1a** and **1c** with electrophiles was also studied, by using *n*-butyl iodide under neutral conditions. The introduction of butyl groups increases the solubility of the bis-betaines in organic solvents, and the *N*-alkylated systems may be suitable models for the study of their stability under basic conditions. In this context, extensive investigation of the formation of stable carbenes from imidazolium quaternary salts has been carried out.[6] The imidazolium quaternary units are stable in 1-alkyl-3-(1*H*-azolylmethyl)imidazolium salts,[5a] and their homologues, and also in analogous and macrocyclic systems. Thus, the putative formation of by-products through the generation of imidazol-2-ylidenes has not been detected to date.[5b]

Abstract in Catalan: *Guiats pel coneixement adquirit en la selecció prèvia de blocs fonamentals amb natura de betaïna per a la construcció d'heterofans quadrupolars, en aquest treball es descriu una estratègia sintètica de tipus convergent "3+1" per a la síntesi dels esmentats macrocicles construïts a partir de subunitat(s) de betaïna, constituint el primer exemple de ciclofans formats per unitats heteroaromàtiques π-excedents i π-deficients unides en disposició 1,3-alternant. La reactivitat química dels heterofans quadrupolars* ***1a*** *i* ***c*** *enfront electròfils en condicions neutres confirma la seva estructura de bis-betaïna. Les característiques estructurals de les bis-betaïnes* ***1****, betaïnes* ***2***·PF_6*,* ***5***·*X i els corresponents* $[1_4]$*heterofans dicatiònics* ***3***·*2X,* ***4***·*2Cl van ser estudiades mitjançant espectroscòpia de* ^1H *i* ^{13}C *NMR com també spectrometria de masses d'ionització per electrosprai, i confirmades per anàlisi de difracció de raigs-X dels macrocicles* ***1a*** *i* ***2a***·PF_6.

Results and Discussion

Synthesis: The synthetic route to the *meta*-heterophanes **4a**·2Cl and **4b**·2Cl involves a "3+1" convergent synthesis based on the coupling of protophanes **6a** and **6b** with the bis-chloromethyl derivative **7**[7] in acetonitrile under reflux. The *N*-benzhydryl macrocyclic dications **4a**·2Cl and **4b**·2Cl were obtained in good yields through a clean macrocyclization reaction (Scheme 2).

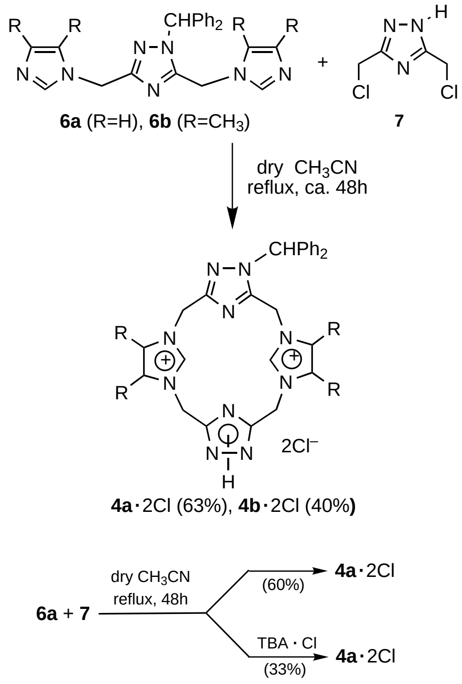

Scheme 2. "3+1" convergent synthesis of dicationic $[1_4]$heterophanes **4a**·2Cl and **4b**·2Cl.

This "3+1" convergent, stepwise synthesis of several examples of dicationic $[1_4]$heterophane frameworks containing two imidazolium rings (such as **3**·2X) is template-controlled in the presence of anions. Moreover, the molecular recognition motifs for anion templating involve the interaction of a multicentered chloride ion with the heteroaromatic and aromatic rings as hydrogen-bond donors (chloride anions selectively increased the yield, which was very low with other anions such as PF_6^-[8]). Accordingly, the macrocyclization reaction leading to the *N*-benzhydryl macrocyclic dication **4a**·2Cl was examined (Scheme 2).

The "3+1" stepwise synthesis based on the coupling of the trinuclear *N*-benzhydryl protophane **6a** with 3,5-bis(chloromethyl)-1,2,4-triazole (**7**) was not anion-dependent. Under standard reaction conditions with equivalent amounts of the reagents at 2.3 mM in dry acetonitrile,[8] coupling between **6a** and **7** produced the dication **4a**·2Cl in 60% yield; this decreased to 33% when five equivalents of tetrabutylammonium chloride were added. An increase in the initial concentrations of the starting materials **6a** and **7** to 8 mM produced the dication **4a**·2Cl in 66% yield. This 6% increase supports the idea of conformationally biasing assistance and of the reaction not being anion-controlled. Both the condensation step and the ring-closure step imply quaternization of the azaaromatic compound **6a** through a Menschutkin type reaction. The "3+1" approach was governed by stereoelectronic control due to the *N*-benzhydryl group in protophane **6a**.

Transformation of dicationic $[1_4]$heterophanes **4a**·2Cl and **4b**·2Cl into betaines **5a**·X and **5b**·X was carried out with an Amberlite IRA-401 anion-exchange resin (OH^- form). The eluates containing macrocycles **5a**·OH and **5b**·OH were carefully acidified to pH 6–7 with either $HCl-H_2O$ or HPF_6-H_2O (Scheme 3); macrocyclic intermediates **5a**·OH and **5b**·OH were characterized by ^1H NMR, despite their instability.

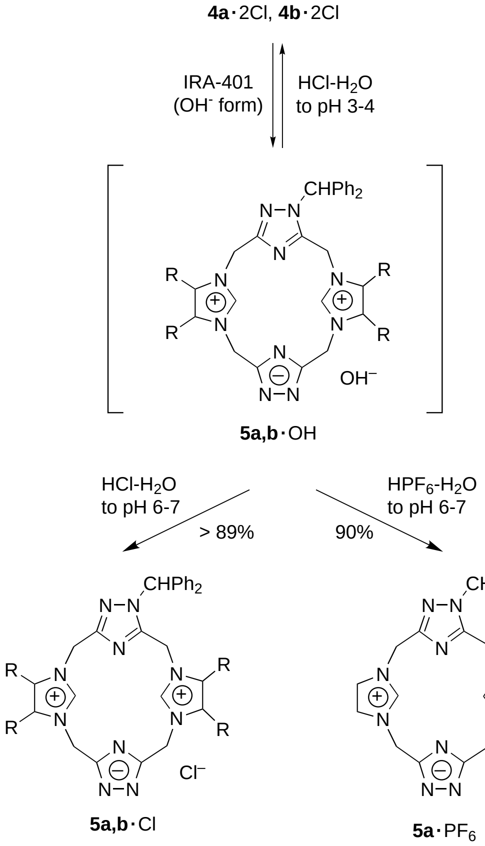

Scheme 3. Synthesis of macrocyclic betaines **5** from dicationic **4a**·2Cl and **4b**·2Cl.

Removal of the benzhydryl group by hydrogenolysis failed with either palladium or palladium hydroxide under standard conditions. The *N*-benzhydryl group was, however, removed by treatment of macrocycles **4a**·2Cl and **4b**·2Cl with trifluoroacetic acid, and pure bis-trifluoroacetates **3a**·$2CF_3CO_2$ and **3b**·$2CF_3CO_2$ were obtained. Through use of Amberlite IRA-401 anion-exchange resin (OH^- form), dications **3a**·$2CF_3CO_2$ and **3b**·$2CF_3CO_2$ were then transformed almost quantitatively into the bis-betaines **1a** and **1b**, and subsequent acidification to pH 6–7 with an aqueous solution of HPF_6 afforded betaines **2a**·PF_6 and **2b**·PF_6. The pH range is not the same as for the corresponding building blocks; acidic treatment of bis-betaines **1a** and **1b** at pH 3–4 produced the bis-hexafluorophosphate dications **3a**·PF_6 and **3b**·PF_6,[4b] while acidification of the betaine subunit to form the corresponding *N*-(1*H*-1,2,4-triazolylmethyl)imidazolium proceeded at pH ≈6.[5a]

Pure dicationic $[1_n]$heterophanes are hard to isolate when the solubility of the ionic species also present in the reaction mixture is similar.[1, 4] A key feature of the current synthetic route, shown in Scheme 4, is the purity of the dicationic macrocycles **3a**·$2CF_3CO_2$ and **3b**·$2CF_3CO_2$, owing to the fact that the trifluoroacetate counterions increased the solubility of the dications in organic solvents and facilitated their purification. Accordingly, it was possible to grow crystals of bis-betaine **1a** and betaine **2a**·PF_6 suitable for X-ray diffraction analysis (see later).

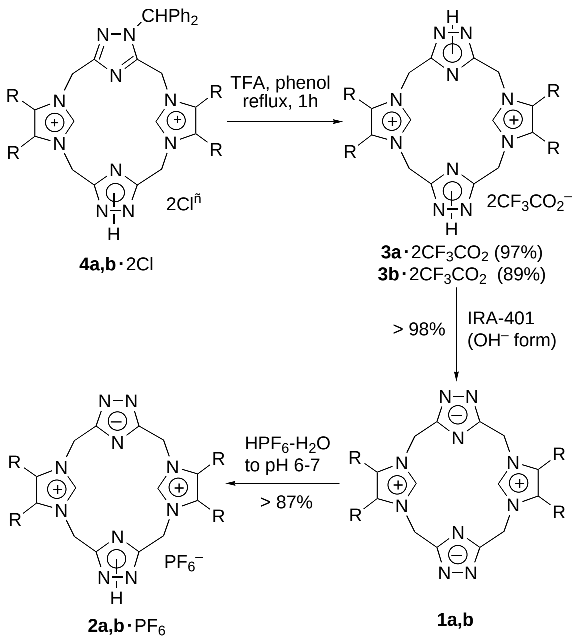

Scheme 4. Deprotection of **4a**·2Cl and **4b**·2Cl and access to macrocyclic betaines **2**·PF_6 and bis-betaines **1** from dicationic **3**·$2CF_3CO_2$.

Reactivity toward electrophiles: *N*-Alkylation of bis-betaines **1a** and **1c** was carried out with an excess of *n*-butyl iodide under neutral conditions; the different experiments are listed in Table 1 (Scheme 5). Initially, the yield of *N*-alkylation of the bis-betaine **1a** was fairly low (27%), probably due to the low solubility of bis-betaine **1a** in organic solvents. From various *N*-alkylation assays, the best result obtained was by using 10 equivalents of *n*-butyl iodide in acetonitrile under reflux for 48 h (42%). *N*-Alkylation of bis-betaine **1c** gave 77% yield, which is in accordance with the betaine nature of the macrocyclic framework.

Table 1. *N*-alkylation reactions of bis-betaines **1a** and **1c** with *n*-butyl iodide.

Assay	Starting material	[**1a**, **1c**]/[BuI] [mol]	Solvent	Reaction time [h]	Products [%][a] **8a**, **c** or **9a**, **c**	**1a**, **c**
1	**1a**	1/5	CH_3CN[b]	48	27	52
2	**1a**	1/5	DMF[c]	112	[d]	[d]
3	**1a**	1/10	CH_3CN[b]	48	42	18
4	**1a**	1/10	CH_3CN[b]	54	48[e]	11
5	**1a**	1/10	EtOH[b]	29	< 42	30
6[f]	**1a**	1/10	CH_3CN[b]	48	44	–
7	**1c**	1/5	CH_3CN[b]	4	77	–

[a] Yield of isolated compound and recovered starting material. [b] Temperature: reflux. [c] At 80 °C. [d] Complex mixture, not fully characterized. [e] Difficult isolation, due to the presence of by-products. [f] Soxhlet system.

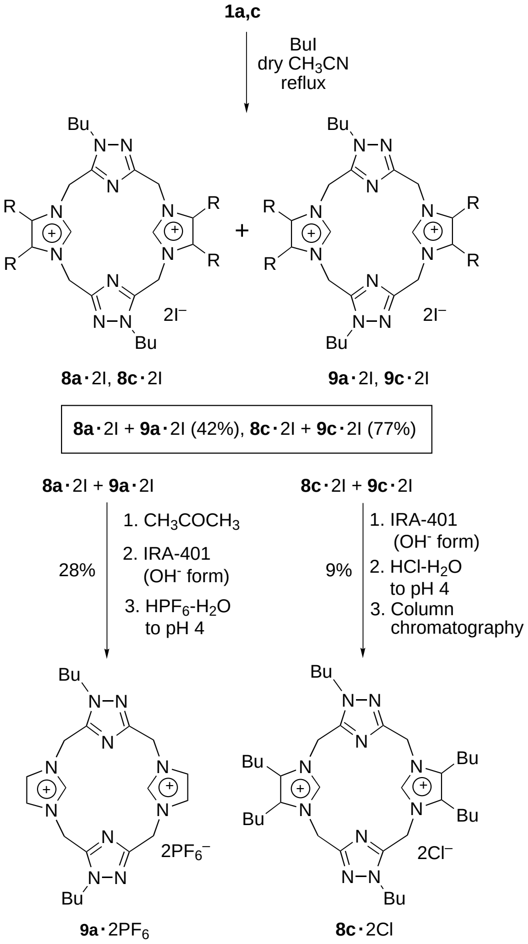

Scheme 5. Reactivity of quadrupolar heterophanes **1** towards butyl iodide.

As products of the *N*-alkylation reaction, isomeric macrocyclic dications **8a**·2I/**8c**·2I and **9a**·2I/**9c**·2I were obtained in statistical ratio, while yields were variable since the *N*-alkylated dications were hard to isolate. After many trials, isomer **9a**·2I was isolated and subsequently converted to the hexafluorophosphate salt **9a**·$2PF_6$, whereas isomer **8c**·2I was isolated as its dichloride salt **8c**·2Cl (Scheme 5).

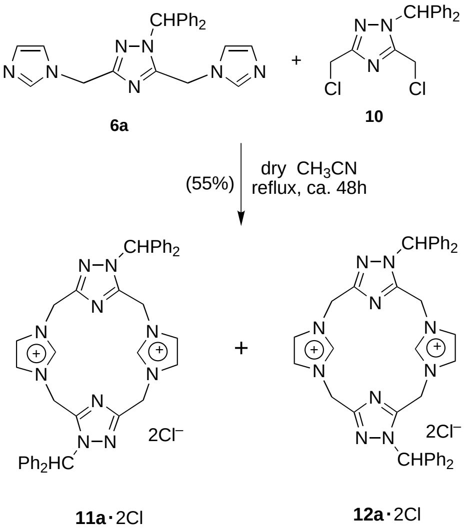

Scheme 6. "3+1" Convergent synthesis of isomeric dicationic [1_4]heterophanes **11**·2Cl and **12**·2Cl.

In view of the accessibility of the trinuclear protophane **6a** and the *N*-benzhydryl-3,5-bis(chloromethyl)derivative **10** as starting materials, we decided to apply a "3+1" convergent synthesis to the preparation of dialkylated compounds **11a**·2Cl and **12a**·2Cl (Scheme 6). By following the standard protocol the two isomers **11a**·2Cl and **12a**·2Cl were produced in statistical ratio, and pure compound **11a**·2Cl was isolated.

Physical data of all the new compounds reported are listed in Table 2, except for 3-methyl-1-imidazoliomethyl-3(5)pyrazolate, which is reported in the Supporting Information.

Spectroscopic methods: The structures of the novel heterophanes **1**–**5**, **8**, **9**, **11**, and **12** were determined by spectroscopy. The IR spectra of compounds **4a**·2Cl and **4b**·2Cl showed one absorption band in the range 3200–3000 cm^{-1} ($\tilde{\nu}_{NH}$), while this band was not seen for betaines **5a**·Cl, **5b**·Cl, and **5a**·PF_6. Dications **3a**·$2CF_3CO_2$ and **3b**·$2CF_3CO_2$ also showed absorption bands in the 3200–3000 cm^{-1} range ($\tilde{\nu}_{NH}$), as well as a band in the 1750–1650 cm^{-1} range ($\tilde{\nu}_{CO}$) corresponding to the trifluoroacetate counterions. Absorptions at 3100 cm^{-1} ($\tilde{\nu}_{NH}$) and 850 cm^{-1} ($\tilde{\nu}_{PF6}$) were shown by dipolar heterophanes **2a**·PF_6, **2b**·PF_6, and **5a**·PF_6, while these bands were not seen with the bis-betaines **1a** and **1b**.

Table 2. Physical data of macrocyclic compounds.

Compound[a]	Yield [%][b]	m.p. [°C] (solvent)[c]	Time [h][d]	Molecular formula[e]
1a	97	> 300 (EtOH)	[f]	$C_{14}H_{14}N_{10}\cdot 4H_2O$
1b	98	> 300	[f]	[g]
2a·PF_6	87	[h] (*i*PrOH/H_2O)	[f]	$C_{14}H_{15}N_{10}PF_6$
2b·PF_6	85	[h]	[f]	[g]
3a·$2CF_3CO_2$	97	208	1	$C_{18}H_{16}N_{10}F_6O_4\cdot 2H_2O$
3b·$2CF_3CO_2$	89	[h]	1	[f]
4a·2Cl	63	> 300	48	$C_{27}H_{26}N_{10}Cl_2\cdot 0.5H_2O$
4b·2Cl	40	230 (CH_3CN/CH_3OH)	48	$C_{31}H_{34}N_{10}Cl_2\cdot 5H_2O$
5a·Cl	90	228	[f]	$C_{27}H_{25}N_{10}Cl\cdot 4H_2O$
5b·Cl	89	[h]	[f]	$C_{31}H_{33}N_{10}Cl_2\cdot 5H_2O$
8c·2I	6	262–264	[f]	$C_{38}H_{64}N_{10}I_2$
9a·2I	17	228–230	[f]	$C_{22}H_{32}N_{10}I_2\cdot 0.5H_2O$
11a·2Cl	14	> 300	[f]	$C_{40}H_{36}N_{10}Cl_2\cdot 0.5H_2O$

[a] TLC: silica gel, solvent system CH_3OH/NH_4Cl(2M)/CH_3NO_2 (6:3:1). [b] Yields were not optimized. [c] Recrystallization solvent. [d] Reaction temperature: reflux. [e] Satisfactory analytical data (±0.4% for C, H, N). [f] See Experimental Section. [g] Not analyzed. [h] Hygroscopic solid.

0947-6539/02/0802-0477 $ 17.50+.50/0

NMR Spectroscopy: Both the ^{1}H and the ^{13}C NMR chemical parameters were crucial for assessing the dipolar and quadrupolar natures of the compounds, as they had been for their corresponding dipolar building blocks[5a] (see Tables 3–6, below). Assignments were made by using NMR experiments (ROESY, HMQC, and HMBC). Figure 1 illustrates the key NMR responses for dication **4a**·2Cl, except for the NH proton in the 1,2,4-triazole subunit.

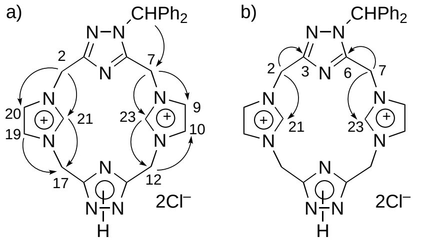

Figure 1. Key NMR responses for heterophane **4a**·2Cl: a) ROESY experiment, and b) HMBC correlation.

The ^{1}H and ^{13}C NMR data for betaines **5a**·X and **5b**·X and for their corresponding dichloride salts **4a**·2Cl and **4b**·2Cl are listed in Table 3 (see Figure 1); the observed shielding effect provides evidence of charge distribution in the dipolar macrocyclic system. Comparison of the proton chemical shifts of betaines **5a**·X and **5b**·X with those of their precursors **4a**·2Cl and **4b**·2Cl reveals that the δ values of CH_2-12, CH_2-17, H-21, and H-23 from the imidazolium rings shift upfield (see Table 3). Despite the instability of betaine **5a**·OH, it was possible to record the ^{1}H NMR spectrum in [D$_6$]DMSO, and a major shielding effect was observed: for example, $\Delta\delta H-12,17 \approx 0.32$ ppm and $\Delta\delta H-21,23 \approx 0.21$ ppm. In D_2O, **5a**·OH showed H/D exchange for the imidazolium acidic hydrogen atoms at positions 21 and 23.

In contrast to what happened with the methyleneimidazolium triazolate building blocks[5a] (see also 3-methyl-1-imidazoliomethyl-3(5)pyrazolate in the Supporting Information), this is the first time that the tendency to hydration has been minimized. The NMR spectra recorded in D_2O were reliable, and the chemical shift variation between betaines **5a**·Cl and **5b**·Cl and their corresponding dications **4a**·2Cl and **4b**·2Cl showed a shielding effect. For example, the betaine **5a**·Cl showed an average shielding of −0.32 ppm for the methylene hydrogen atoms and of −0.21 ppm for H−21,23 in the imidazolium rings (see $\Delta\delta$ in Table 3). As far as betaine **5a**·PF_6 is concerned, the shielding effect was indeed more pronounced, especially in [D$_6$]DMSO, in which the chemical shifts of **5a**·PF_6 were like those for betaine **5a**·OH. This indicates the presence of weaker interactions between the dipolar [1$_4$]heterophane framework and the counteranion in the relative order $OH^- \cong PF_6^- > Cl^-$ (see Table 3 and X-ray crystallography).

Table 3. Selected ^{1}H NMR and ^{13}C NMR data for betaines **5a**·X and **5b**·X and their corresponding dichloride salts **4a**·2Cl and **4b**·2Cl.

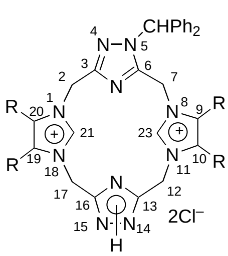

4a,b·2Cl

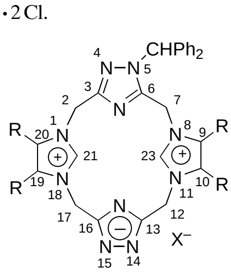

5a,b·X

Compound	Solvent	H-21	H-23	H-2	H-7	H-12	H-17
5a·OH[a]	[D$_6$]DMSO	8.91	9.07	5.45	5.87	5.35	5.30
5a·Cl	[D$_6$]DMSO	9.05	9.16	5.48	5.98	5.52	5.52
4a·2Cl[b]	[D$_6$]DMSO	9.16	9.25	5.56	5.97	5.66	5.63
	$\Delta\delta$[c]	−0.25	−0.18	−0.11	−0.10	−0.31	−0.33
	$\Delta\delta$[d]	−0.11	−0.09	−0.08	+0.01	−0.14	−0.11
5a·Cl	D_2O	8.41	8.67	5.38	5.49	5.28	5.25
4a·2Cl	D_2O	8.64	8.86	5.29	5.37	5.52	5.48
	$\Delta\delta$[d]	−0.23	−0.19	−0.09	−0.12	−0.24	−0.23
5a·PF_6	[D$_6$]DMSO	8.90	9.10	5.46	5.88	5.35	5.32
4a·2Cl[b]	[D$_6$]DMSO	9.16	9.25	5.56	5.97	5.66	5.63
	$\Delta\delta$[e]	−0.26	−0.15	−0.10	−0.09	−0.31	−0.34
5a·PF_6	D_2O	8.43	8.69	5.39	5.48	5.29	5.24
4a·2Cl	D_2O	8.64	8.86	5.29	5.37	5.52	5.48
	$\Delta\delta$[e]	−0.21	−0.17	−0.10	−0.11	−0.23	−0.24
5b·Cl	[D$_6$]DMSO	9.00	9.04	5.47	5.91	5.43	5.43
4b·2Cl[b]	[D$_6$]DMSO	9.15	9.15	5.52	5.94	5.59	5.59
	$\Delta\delta$[b]	−0.15	−0.11	−0.05	−0.03	−0.16	−0.16
4b·2Cl	D_2O	8.48	8.69	5.17	5.27	5.35	5.35
		C-21	C-23	C-2	C-7	C-12,17	
5a·PF_6	D_2O	135.2	135.2	51.1	53.0	53.0	
5a·Cl	[D$_6$]DMSO	137.6	138.4	45.9	44.2	46.9	
4a·2Cl[f]	[D$_6$]DMSO	138.4	138.9	46.1	44.3	45.4	
	$\Delta\delta$[g]	−0.8	−0.5	−0.2	−0.1	+1.5	
5b·Cl	[D$_6$]DMSO	136.4	136.7	43.8	41.8	43.7	
4b·2Cl[f]	[D$_6$]DMSO	137.0	137.0	43.8	42.0	42.5	
	$\Delta\delta$[g]	−0.6	−0.3	0	−0.2	+1.2	

[a] Compound unstable in [D$_6$]DMSO. [b] Assignation of signals by ROESY. [c] $\Delta\delta$: observed chemical shift differences between compound **5a**·OH and the macrocycle **4a**·2Cl. [d] $\Delta\delta$: observed proton chemical shift differences between betaines **5a**·Cl and **5b**·Cl and the macrocycles **4a**·2Cl and **4b**·2Cl ($\delta_{betaine} - \delta_{macrocycle}$). [e] $\Delta\delta$: observed proton chemical shift differences between betaine **5a**·PF_6 and the macrocycle **4a**·2Cl ($\delta_{betaine} - \delta_{macrocycle}$). [f] Assignation of signals by HMBC and HMQC. [g] $\Delta\delta$: observed ^{13}C chemical shift differences between betaines **5a**·Cl and **5b**·Cl and the macrocycles **4a**·2Cl and **4b**·2Cl ($\delta_{betaine} - \delta_{macrocycle}$).

For bis-betaines **1a** and **1b**, betaines **2a**·PF_6 and **2b**·PF_6, and dications **3a**·2CF_3CO_2 and **3b**·2CF_3CO_2, the ^{1}H NMR spectra (20 °C) in several solvents showed sharp singlets for the bridging protons (Table 4); this indicated a high degree of conformational flexibility[4]; dynamic NMR experiments were precluded due to the compounds' high insolubilities. In bis-betaines and betaines a clear shielding effect was observed, especially for the methylene spacers and $\delta H-21(23)$ (Im+) (see $\Delta\delta H$ in Table 4). For example, the differences in the chemical shifts of bis-betaine **1a** and dication **3a**·2CF_3CO_2 in CD_3OD were $\Delta\delta CH_2 = -0.27$ ppm and $\Delta\delta H-21,23 = -0.73$ ppm, while in betaine **2a**·PF_6 they were $\Delta\delta CH_2 = -0.18$ ppm and $\Delta\delta H-21,23 = -0.54$ ppm.

For compounds **1a**, **2a**·PF_6, and **3**·2CF_3CO_2, the ^{1}H NMR spectra in CD_3OD showed identical chemical shifts on

Table 4. ^1H NMR data for bis-betaines **1a** and **1b**, betaines **2a**$\cdot PF_6$ and **2b**$\cdot PF_6$, and dications **3a**$\cdot 2\,CF_3CO_2$ and **3b**$\cdot 2\,CF_3CO_2$.

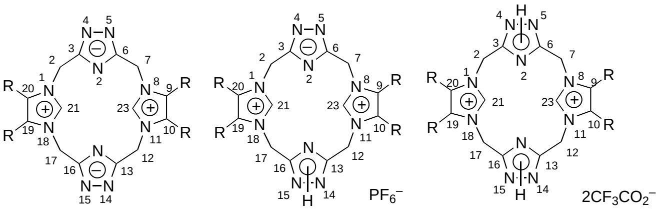

1a,b **2a,b**$\cdot PF_6$ **3a,b**$\cdot 2CF_3CO_2$

Compound	Solvent	H-2,7,12,17	H-21, 23	R
1a	D_2O	5.19	7.91	7.42
2a$\cdot PF_6$	D_2O	5.33	8.34	7.45
3a$\cdot 2\,CF_3CO_2$	D_2O	5.45	8.78	7.45
$\Delta\delta$[a]		– 0.26	– 0.87	– 0.03
$\Delta\delta$[b]		– 0.14	– 0.43	0
1a	[D$_6$]DMSO	5.28	8.79	7.79
2a$\cdot PF_6$	[D$_6$]DMSO	5.48	8.99	7.80
3a$\cdot 2\,CF_3CO_2$	[D$_6$]DMSO	5.61	9.12	7.81
$\Delta\delta$[a]		– 0.33	– 0.33	– 0.02
$\Delta\delta$[b]		– 0.20	– 0.20	– 0.01
1a	CD_3OD	5.46	8.66	7.80
2a$\cdot PF_6$	CD_3OD	5.55	8.85	7.80
3a$\cdot 2\,CF_3CO_2$	CD_3OD	5.73	9.39	7.80
$\Delta\delta$[a]		– 0.27	– 0.73	0
$\Delta\delta$[b]		– 0.18	– 0.54	0
1a	CD_3OD[c]	5.72	9.38	7.79
2a$\cdot PF_6$	CD_3OD[c]	5.71	9.36	7.74
3a$\cdot 2\,CF_3CO_2$	CD_3OD[c]	5.71	9.36	7.74
$\Delta\delta$[a]		0.01	0.02	0.05
$\Delta\delta$[b]		0	0.02	0
1b	D_2O	5.05	7.87	2.00
2b$\cdot PF_6$	D_2O	5.17	8.23	1.98
1b	[D$_6$]DMSO	5.10	8.32	2.30
3b$\cdot 2\,CF_3CO_2$	[D$_6$]DMSO	5.52	8.99	2.14
$\Delta\delta$[a]		– 0.42	– 0.67	0.16

[a] $\Delta\delta$: Observed proton chemical shift differences between bis-betaines **1a** and **1b** and the macrocycles **3a**$\cdot 2\,CF_3CO_2$ and **3b**$\cdot 2\,CF_3CO_2$ ($\delta_{\text{bis-betaine}} - \delta_{\text{macrocycle}}$). [b] $\Delta\delta$: Observed proton chemical shift differences between betaines **2a**$\cdot PF_6$ and **2b**$\cdot PF_6$ and the macrocycles **3a**$\cdot 2\,CF_3CO_2$ and **3b**$\cdot 2\,CF_3CO_2$ ($\delta_{\text{betaine}} - \delta_{\text{macrocycle}}$). [c] 5% TFA was added.

Table 5. ^1H NMR data for bis-betaine **1a** at several pH values[a] and ^1H NMR chemical shifts of bis-betaine **1a**, betaine **2a**$\cdot PF_6$, and macrocycle **3a**$\cdot 2\,CF_3CO_2$ at different concentrations.

Compound	Solvent	pH	H-2,7,12,17	H-21,23	H- 9,10,19,20
1a	[D$_6$]DMSO	8	5.28	8.79	7.79
		6	5.48	8.99	7.80
		5	5.50	9.03	7.80
		4	5.61	9.12	7.80
		2	5.61	9.12	7.80
		$\Delta\delta$[b]	– 0.33	– 0.33	– 0.01
1a	D_2O	8	5.19	7.90	7.42
		6	5.35	8.44	7.44
		5	5.42	8.68	7.44
		4	5.44	8.75	7.44
		$\Delta\delta$[b]	– 0.26	– 0.87	– 0.06
		Conc. [mM]			
1a	D_2O	4.83 – 30.53	5.19	[c]	7.42
2a$\cdot PF_6$		4.89 – 47.91	5.33	[c]	7.43
3a$\cdot 2\,CF_3CO_2$		4.88 – 64.67	5.43	8.75	7.43

[a] Acidification with 1% aqueous hexafluorophosphoric acid. [b] $\Delta\delta$: Observed proton chemical shift differences between pH 8 and pH 4 ($\delta_{pH\,8} - \delta_{pH\,4}$). [c] Signal not observed due to H/D exchange.

addition of 5% trifluoroacetic acid as a result of the conversion of bis-betaines **1** and betaines **2** into their corresponding bistrifluoroacetates **3**$\cdot 2\,CF_3CO_2$. Table 5 shows ^1H NMR data for bis-betaine **1a** at several pH values. At pH 8, the chemical shifts in [D$_6$]DMSO indicated the presence in solution of the quadrupolar species **1a**, whereas at pH 5 the ^1H δ values corresponded to those of the dipolar macrocycle **2a**$\cdot CF_3CO_2$, which at pH 2 is transformed into the corresponding dication **3a**$\cdot 2\,CF_3CO_2$.

The association behavior of some of the compounds described was examined by NMR, although examination of their complexing properties in solution was hampered by their insolubility. The ^1H NMR spectra of the model compounds **1a**, **2a**$\cdot PF_6$, and **3a**$\cdot 2\,CF_3CO_2$ were recorded at different concentrations at 20 °C in D_2O at 200 MHz. The range of concentrations studied was limited by the low solubilities of the compounds to about 5 to 65 mM (Table 5). From the study we were able to conclude that no significant variation of the chemical shift was observed for any of the protons in macrocycles **1a**, **2a**$\cdot PF_6$, and **3a**$\cdot 2\,CF_3CO_2$; this indicates that aggregates did not form (see below, ESI-MS).

The ^1H NMR data for *N*–dialkylated compounds **8a**$\cdot$2X, **8c**$\cdot$2X, **9a**$\cdot$2X, **9c**$\cdot$2X, **11a**$\cdot$2Cl, and **12a**$\cdot$2Cl showed that isomers **8a**, **8c**, and **11a** could be differentiated from **9a**, **9c**, and **12a**, respectively (Table 6). Thus, for the *anti* isomers **8a**, **8c**, and **11a**, only a singlet signal can be observed for the imidazolium proton atoms H–21 and H–23, whereas two peaks appear for these proton atoms in the *syn* isomers **9a**, **9c**, and **12a**. Individual assignments were made in [D$_6$]DMSO by ROESY for the pure dication **8c**, and by HMBC and HMQC for the pure isomer **11a**$\cdot$2Cl.

The high instability of the pyrazole derivatives in solution, especially the betaines of methyleneimidazolium pyrazolate, obliged us to record the ^{13}C NMR in CD_3OD (see Supporting Information) although, due to solvation, this is not the solvent of choice in which to observe the chemical differences between betaines and their corresponding salts.

Electrospray ionization mass spectrometry: ESI-MS was used to examine multicharged [1$_4$]*meta*-heterophanes in the gas phase. Bis-betaines **1** (M), betaines **2**$\cdot PF_6$ (MH$\cdot$X) and macrocyclic dications **3**$\cdot$2X (MH$_2\cdot$2X) produced clean positive ion ESI mass spectra, and several informative peaks arose from proton transfer reactions with, for example, **1a**, **2a**$\cdot PF_6$, and **3a**$\cdot 2\,CF_3CO_2$ (Table 7). The two common characteristic peaks were the ions $[M{+}H_2]^{2+}$ and $[M{+}H]^{+}$, which resulted from the stepwise protonation of bis-betaines **1**, whilst in betaines **2**$\cdot PF_6$ they were attributed to dissociation of the counterion and protonation. For dications **3**$\cdot$2X, the charged species may be formed by the loss of the two counterions and deprotonation. When the cone voltage was varied from 50 V to 100 V, formation of stable noncovalent polymolecular self-assembled aggregates was observed, especially for the macrocyclic bis-betaines **1**.[9]

From dications **3**$\cdot$2X (MH$_2\cdot$2X) with two proton-ionizable 1,2,4-triazole rings, the model dicationic [1$_4$]*meta*-imidazoliophanes (M$\cdot$2X) that have two aromatic rings and maintain the two imidazolium quaternary moieties have been examined by ESI-MS; the three common ions were $[M]^{2+}$, $[M{+}X]^{+}$

Table 6. Selected ^1H NMR data for compounds **8a**·2X, **8c**·2X, **9a**·2X, **9c**·2X, **11a**·2Cl, and **12a**·2Cl.

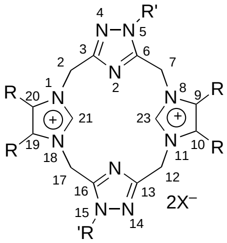

8a,c·2X, **11a**·2Cl

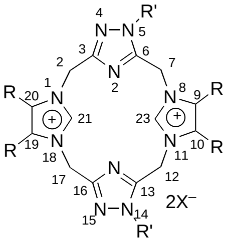

9a,c·2X, **12a**·2Cl

	R	R'
8a·2X, **9a**·2X	H	Bu
8c·2X, **9c**·2X	Bu	Bu
11a·2Cl, **12a**·2Cl	H	$CHPh_2$

Compound	Solvent	H-2,12	H-7,17	H-21,23	
8a·2I[a]	CD_3OD	5.64	5.91	9.40	
8a·2I[a]	$[D_6]DMSO$	5.56	5.80	9.15	
8c·2I[a]	CD_3OD	5.52	5.80	9.16	
8c·2I[a,b]	$[D_6]DMSO$	5.50	5.76	9.02	
8c·2Cl	CD_3OD	5.53	5.80	[c]	
11a·2Cl	$[D_6]DMSO$	5.59	5.96	9.29	
		H-2,17	H-7,12	H-21	H-23
9a·2I	CD_3OD	5.61	5.95	9.38	9.38
9a·2I	$[D_6]DMSO$	5.53	5.84	9.12	9.21
9a·2PF_6	CD_3OD	5.59[d]	5.90	9.31	9.31
9c·2I[e]	CD_3OD	5.50	5.85	9.12	9.20
9c·2I[e]	$[D_6]DMSO$	5.48	5.78	8.96	9.04
9c·2Cl[e]	CD_3OD	5.53	5.84	[c]	[c]
12a·2Cl[f]	$[D_6]DMSO$	5.61	6.05	9.20	9.36

[a] Chemical shift values from enriched samples of compounds **8a**·2X and **8c**·2X (**8a**, **c**·2X/**9a**, **c**·2X 90:10). [b] Assignment of signals by ROESY. [c] Signal not observed, due to H/D exchange. [d] Broad signal. [e] Signals assigned from the difference between spectra corresponding to the mixture of **8c**·2I and **9c**·2I and to the isomer **8c**·2I. [f] Chemical shift values from an enriched sample of compound **12a**·2Cl (**11a**·2Cl/**12a**·2Cl 33:66).

Table 7. Summary of data obtained from positive ion ESI-MS of **1a**, **2a**·PF_6, **3a**·2CF_3CO_2, **9a**·2PF_6, and **11a**·2Cl[a]

V_c [V]	Compound (M_W)	Ions, *m*/*z* ratio Relative abundance [%]				
		$[M+H_2]^{2+}$	$[Pp \cdot H]^{+}$[b]	$[M+H]^{+}$	$[M+H_2+X]^{+}$	$[2M+H]^{+}$
	1a[c] (322.2)	162.2	230.3	323.3	–	645.7
50		**100**	[d]	14	–	2
100		36	82	**100**	–	32
	2a·PF_6[c] (468.3)	162.2	230.3	323.3	469.3	645.7
50		**100**	[d]	4	[d]	<1
100		**100**	44	64	[d]	9
	3a·2CF_3CO_2[c] (550.4)	162.2	230.3	323.3	437.4	645.7
50		**100**	[d]	10	16	<1
100		35	49	**100**	[d]	12
		$[M]^{2+}$	$[M-H]^{+}$	$[M+X]^{+}$	$[M-CHPh_2]^{+}$	
	9a·2PF_6 (726.5)	218.3	435.6	581.5	–	
60		**100**	5	20	–	
80		15	15	**100**	–	
100		5	30	15	–	
	11a·2Cl[e] (727.7)	328.0	655.1	692.9	489.0	
60		17	20	24	**100**	

[a] Molecular weight (M_W) and ion *m*/*z* values apply to the lowest mass component of any isotope distribution and are based on a scale in which $^{12}C = 12.000$. [b] Protophane (Pp, M_W 229.2). [c] **1a** and **2a**·PF_6 (ref. [9]). [d] No signal observed. [e] $[M-H+2H_2O]^+$ at *m*/*z* 691.1 (46%).

and $[M-H]^+$. Accordingly, direct electrospray mass spectrometric evidence was obtained for the singly charged imidazolylidene species $[M-H]^+$; this peak also appeared in the ESI mass spectra of the regiospecific deuterated counterparts as the ion $[M-D]^+$.[5b]

In the present study, the positive-ion ESI-MS of dications **9a**·2PF_6 and **11a**·2Cl were measured as described elsewhere,[5b, 9] samples being dissolved in H_2O/CH_3CN (1:1) at a concentration of 250 pmol µL^{-1}, while the cone voltage was varied between 50 V and 100 V (Table 7). The positive-ion ESI responses of **9a**·2PF_6 (M·2X) and **11a**·2Cl (M·2X) showed the formation of the characteristic ions $[M]^{2+}$ and $[M+X]^+$ together with the carbene species $[M-H]^+$; this result is comparable to those found with $[1_4]$*meta*-imidazoliophanes (M·2X) mentioned above.

The comparative ESI-MS study with bis-betaine **1a**, betaine **2a**·PF_6, and dication **3a**·2CF_3CO_2, together with the *N*-alkylated dications **9a**·2PF_6 and **11a**·2Cl, showed that the π-rich heteroaromatic rings direct their electrospray ionization, changing the nature of the common characteristic peaks (Table 7). Dicationic macrocycle **3a**·2CF_3CO_2 and *N*-butyl dication **9a**·2PF_6 gave clean ESI mass spectra at a cone voltage of ≤60 V (Figure 2), while the base peak of the *N*-benzhydryl dication **11a**·2Cl corresponds to the singly charged ions $[M-CHPh_2]^+$ at *m*/*z* 489, arising from molecular fragmentation. As far as **9a**·2PF_6 (M·2X) and **11a**·2Cl (M·2X) are concerned, the singly charged imidazolylidene species $[M-H]^+$ were produced with a relative abundance ≤20% ($V_c \leq 60$ V).

At a cone voltage of 100 V, macrocycles **1a** and **2a**·PF_6 and the proton-ionizable dication **3a**·2CF_3CO_2 produced two common peaks, together with a singly charged fragment ion $[Pp \cdot H]^+$, due to the protonated trinuclear 3,5-bis(1-imidazolylmethyl)-1*H*-1,2,4-triazole, at *m*/*z* 230.3. A self-assembled aggregate was formed as a singly charged dimer $[2M+H]^+$ at *m*/*z* 645.57, especially in the case of bis-betaine **1a** (32%). At this cone voltage, the dication **9a**·2PF_6 (M·2X) generated the ions $[M-H]^+$ with a relative abundance of 30%.

X-Ray crystallography: One instance of a crystal and molecular structure of a quadrupolar $[1_4]$(*meta*–*ortho*)azolophane (M·4H_2O) has been reported previously.[10] Particularly interesting is the crystal packing, which is mainly governed by a hydrogen-bonding network and strong intermolecular interactions with water, together with weak

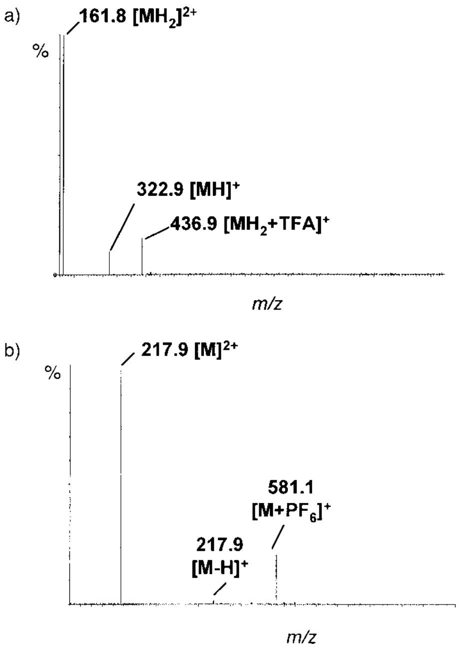

Figure 2. Positive ion ESI-MS of a) dication **3a**$\cdot 2\,CF_3CO_2$ ($V_c = 50$ V) and b) *N*-alkylated dication **9a**$\cdot 2\,PF_6$ ($V_c = 60$ V).

interactions, either intramolecular or with water molecules. The molecular structures of compounds **1a** and **2a**$\cdot PF_6$ described here were confirmed by crystallographic X-ray diffraction.[11] The previously recorded data[4a] were reprocessed with newly available structure-solving and refinement programs and graphical facilities.[11] Figure 3 shows a perspective molecular diagram of quadrupolar heterophane **1a** with the corresponding atom numbering. Since molecule **1a** is a centrosymmetric structure, the experimental asymmetric unit contains a half molecule of **1a** and two water molecules, matched by an equivalent subunit generated by symmetry. Thus, the atom numbering system is not the same as the atom numbering system for the single-crystal X-ray diffraction analysis. For example, the four reference-plane methylene carbon atoms C2 ,C7, C12, and C17 are numbered as C2, C7, C2′, and C7′, respectively.

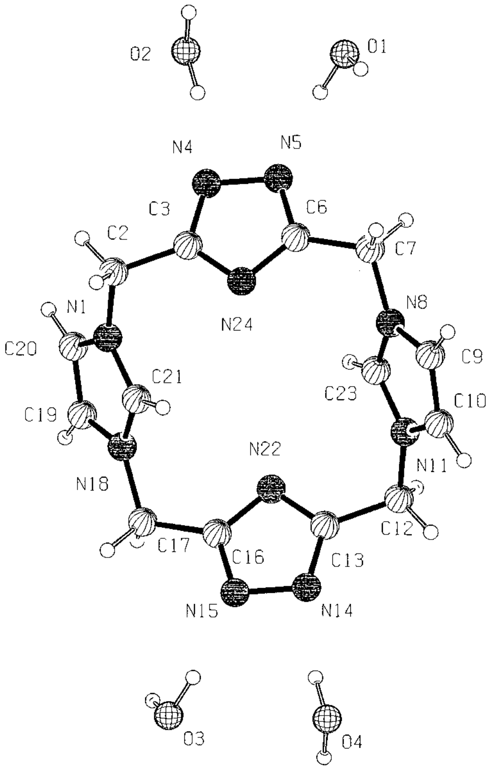

Figure 3. Perspective molecular diagram of quadrupolar heterophane **1a**.

The bond lengths and angles correlate well with those in dipolar compound **2a**$\cdot PF_6$ (vide infra and Table 8), and are close to those described in crown ether structures for the π-excessive rings.[12] The molecular shape may be described by the spatial disposition within the four heteroaromatic planes, by their inclination with respect to the reference plane, and by the macrocyclic dimensions (Table 8). The weighted least-squares plane defined by the C2, C7, C12, and C17 methylene carbon atoms has a side of length 4.96 Å. The C21 and C23 imidazolium carbon atoms as well as the N22 and N24 *s*-triazolate nitrogen atoms are oriented on opposite sides of the reference plane at 0.22 Å and 0.27 Å, respectively. The C21 atom and the N24 atom are located on the upper side of the rim. Significant nonbonding distances [Å] related to the

Table 8. Selected X-ray crystallographic data for bis-betaine **1a** and betaine **2a**$\cdot PF_6$.

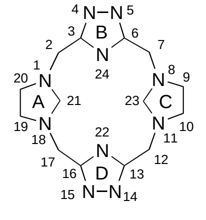

1a

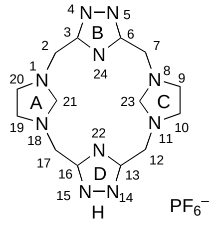

2a$\cdot PF_6$

	1a	**2a**$\cdot PF_6$**A**	**2a**$\cdot PF_6$**B**
C21⋯C23 Å[a]	4.57	4.55	4.38
N22⋯N24 Å[a]	4.29	4.40	4.44
N4⋯N15 Å[a]	7.75	6.90	6.91
N5⋯N14 Å[a]	7.75	6.99	7.00
C2⋯C7 Å[a]	4.94	4.95	4.91
C2⋯C12 Å[a]	6.89	6.95	7.06
C21⋯C9 Å[a]	6.06	6.02	6.06
N1⋯N8 Å[a]	5.60	5.68	5.72
C7⋯C17 Å[a]	7.07	6.97	6.92
A–B [°][b]	118	68	55
A–D [°][b]	118	53	52
A–C [°][b]	0	16	40
A–E [°][b]	49	33	1.6
B–C [°][b]	118	71	67
B–D [°][b]	0	105	106
B–E [°][b]	137	60	55
C–D [°][b]	118	65	61
C–E [°][b]	49	49	41
D–E [°][b]	137	45	52
C21⋯E Å[c]	0.22	0.21	0.06
C23⋯E Å[c]	0.22	0.19	0.17
N22⋯E Å[c]	0.27	0.25	0.29
N24⋯E Å[c]	0.27	0.39	0.34

[a] Most relevant intermolecular distances. [b] Dihedral angles between the weighted least-squares planes. Plane A: C19-N18-C21-N1-C20, Plane B: N4-C3-N24-C6-N5, Plane C: C9-N8-C21-N11-C10, Plane D: C14-C13-N22-C16-N15, Plane E: C2-C7-C12-C17. [c] Distance between the indicated atom and the reference plane E.

macrocyclic dimensions are: N1···N8 5.60(1), C2···C7 4.94(1), C2···C12 6.89(1), N4···N15 7.75(1), C7···C17 7.07(1), C21···C23 4.57(1), N22···N24 4.29(1).

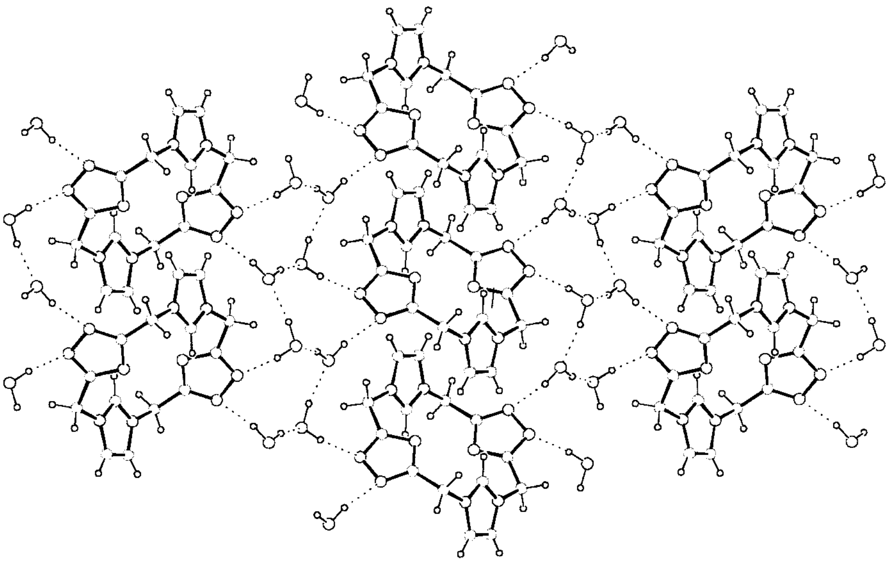

Figure 4. Partial packing diagram illustrating sheet structure of **1a** and showing the water chain formation.

The crystal packing, as illustrated in Figure 4, reveals the solid state structure of compound **1a**. The water molecules sustaining the crystalline network act as both donors and acceptors of hydrogen bonds and are responsible for the formation of corrugated sheets perpendicular to the *ac* plane (Figure 4). These water molecules are held together by O−H···O hydrogen bonds; this results in chains along the *b* axis. Each oxygen is an acceptor of a hydrogen bond from the other independent water molecule: O1−H11···O2 and O2−H21···O1 (Table 9). Both are donors through the other hydrogen atom to the triazole moiety: O1−H12···N5 and O2−H22···N4, thereby joining molecules by translation along the *b* axis and by a twofold screw axis; this forms a layer structure in which alternating ribbons of macrocycles and water molecules are observed. Neighboring layers are staggered; this facilitates the formation of water channels (Figure 4).

Table 9. Hydrogen bonding geometry [Å or °]

D−H	d(D−H)	d(H···A)	⟨DHA	d(D···A)	A
O1−H11	0.989	1.800	173.81	2.785	O2[a]
O1−H12	0.944	1.909	171.76	2.846	N5
O2−H21	0.952	1.849	164.77	2.779	O1[b]
O2−H22	0.989	1.891	170.49	2.872	N4

Symmetry codes: [a] *x*, *y*+1, *z*. [b] −*x*+3/2, *y* − 1/2, −*z*+5/2.

For the dipolar heterophane **2a**·$\mathrm{PF_6}$, the asymmetric unit contains two independent molecules (cations)—**A** and **B**—and their associated hexafluorophosphate counterions.[4a] Bond lengths, angles, and the macrocyclic dimensions of both molecules **2A** and **2B** are similar and correlate well with those observed for **1a**, as shown in Table 8. The main structural difference between molecules **2A**·$\mathrm{PF_6}$ or **2B**·$\mathrm{PF_6}$ in relation to quadrupolar heterophane **1a** is a consequence of the relative spatial disposition of the rings. Noteworthy is the differing orientation of the triazole rings, which are parallel in compound **1a** but almost perpendicular in both the **A** and the **B** molecules of **2a**·$\mathrm{PF_6}$.

The crystal packing shows that the molecules of **2a**·$\mathrm{PF_6}$ dispose themselves so as to form two independent hydrogen-bond networks (Figure 5 and Supporting Information). Both molecules **A** and **B** from neighboring networks are associated mainly through intermolecular N−H···N hydrogen bonds: in the first one, molecules of type **A** are involved, through a N15**A**−H15···N5**A** interaction, and in the second one molecules of type **B** participate through a N15**B**−H15···N5**B** interaction. The $\mathrm{PF_6^-}$ counterions are located in an alternated disposition between molecules; this helps to sustain the crystal lattice, unlike in quadrupolar heterophane **1a**, in which crystal packing was mainly governed by a hydrogen bond network based on water channels.

Conclusion

The quadrupolar macrocycles **1** have emerged as prototypes of nonclassical cyclophanes. An alternative and convenient route to the key dicationic intermediates **3**·2X by deprotection of the *N*-diphenylmethyl dications **4**·2X have been

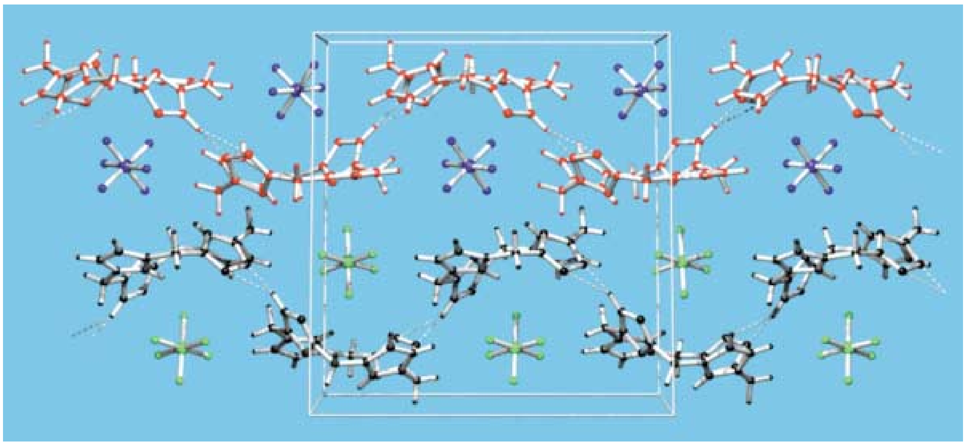

Figure 5. Partial crystal packing along the *a* axis for **2a**·$\mathrm{PF_6}$ showing the two independent hydrogen bond networks.

0947-6539/02/0802-0482 $ 17.50+.50/0

reported. This synthetic pathway has provided bis-betaines **1** and betaines **2**·PF_6, and has become the method of choice for their preparation. The chemical reactivity of bis-betaines **1** toward electrophiles corroborates their quadrupolar structure. Their structural properties have been examined in detail, and ^{1}H NMR studies have provided evidence of the charge distributions in these [1_4]*meta*-heterophane frameworks in solution. These were confirmed in the solid state by single-crystal X-ray analysis of **1a** and **2a**·PF_6. Electrospray ionization revealed the formation of several informative peaks arising from proton-mediated ion–molecule reactions. Among these, stable noncovalent self-assembled aggregates were observed in the gas phase. Efforts are currently being directed toward applications of the betaine building blocks for the construction of supramolecular scaffolds, passing from quadrupolar to multipolar systems.

Experimental Section

General Methods: Melting points: CTP-MP 300 hot-plate apparatus with ASTM 2C thermometer (given in Table 2). IR (KBr disks): Perkin Elmer 1430 spectrophotometer. ^{1}H NMR: Varian Gemini 200 and Varian Unity 300 spectrometers (200 MHz and 300 MHz). ^{13}C NMR: Varian Gemini 200 spectrometer (50.3 MHz). HMQC and HMBC: Varian VXR 500 spectrometer (500 MHz). NMR spectra were determined in [D$_6$]dimethyl sulfoxide, and chemical shifts are expressed in parts per million (proton δ relative to the central peak of [D$_6$]dimethyl sulfoxide. ES-MS: VG-Quattro mass spectrometer. EIMS: Hewlett-Packard HP-5988A and Finnegan TSQ-70. TLC: Merck precoated 60 F254 silica gel plates; solvent systems, detection by UV light. For anion exchange, a column (12.7 mm diameter) was packed with IRA-401 anion-exchange resin (OH^- form)[5a] to a height of 12.7 cm. When a rotary evaporator was used, the bath temperature was 25 °C. In general, the compounds were dried overnight at 25 °C in a vacuum oven. Microanalyses were performed on a Carlo Erba 1106 analyzer.

Materials: Protophanes **6a**[13] and **6b**,[13] 3,5-bis(chloromethyl)-1,2,4-triazole (**7**),[7] and *N*-benzhydryl-3,5-bis(chloromethyl)-1,2,4-triazole (**10**)[13] were prepared as described in the literature.

Bis-betaines 1a and 1b: (Table 2) A column packed with an IRA-401 Amberlite anion-exchange resin was used and the chloride form was converted into the hydroxide form. A solution of macrocycle **3a**·2 CF_3CO_2 (129 mg, 0.23 mmol) in 90% ethanol (60 mL) was passed through the column. The neutral eluates were evaporated to dryness to give the corresponding inner salt **1a**.

Betaines 2a·PF_6 and 2b·PF_6: (Table 2) A solution of bis-betaines **1a** and **1b** (100 mg) in water (50 mL) was acidified to pH 6 with 1% aqueous hexafluorophosphoric acid. The solvent was then evaporated to dryness to give betaines **2a**·PF_6 and **2b**·PF_6.

Macrocycles 3a·2CF_3CO_2 and 3b·2CF_3CO_2: (Table 2) A stirred solution of **4a**·2 Cl (500 mg, 0.9 mmol) or **4b**·2 Cl (500 mg, 0.8 mmol) and phenol (500 mg, 5.3 mmol) in trifluoroacetic acid (10 mL) was heated under reflux for 1 h. The reaction mixture was cooled and the solvent was removed to dryness. The resulting oil was triturated with diethyl ether (4 × 20 mL) and filtered to give the corresponding trifluoroacetates **3a**·2 CF_3CO_2 and **3b**·2 CF_3CO_2.

Attempted preparation of macrocycle 3a·2Cl by hydrogenolysis of 4a·2Cl. Experiment 1: Pd-C (10%, 7 mg, 10% weight) was added to a solution of **4a**·2 Cl (67 mg, 0.1 mmol) in dry methanol (60 mL), and the mixture was hydrogenated at atmospheric pressure and room temperature for 42 h. An extra quantity of Pd-C (10%, 14 mg, 20% weight) was added, and the mixture was further hydrogenated for 67 h. The suspension was filtered, and the solution was evaporated to dryness to recover compound **4a**·2 Cl (49 mg, 70%).

Experiment 2: $Pd(OH)_2$ (20%, 10 mg, 10% weight) was added to a solution of **4a**·2 Cl (70 mg, 0.1 mmol) in dry methanol (60 mL), and the mixture was hydrogenated at atmospheric pressure and room temperature for 5 h. An extra quantity of Pd-C (10%, 24 mg, 20% weight) was added, and the mixture was further hydrogenated for 8 h. The suspension was filtered and the solution was evaporated to dryness to recover compound **4a**·2 Cl (57 mg, 81%)

Macrocycles 4a·2Cl and 4b·2Cl: (Table 2) A stirred solution of 3,5-bis(chloromethyl)-1,2,4-triazole (**7**; 0.5 g, 2.8 mmol) in dry acetonitrile (45 mL) was added dropwise to a solution of 1-benzhydryl-3,5-bis(1-imidazolylmethyl)-1,2,4-triazole (**6a**; 1.1 g, 2.8 mmol) or 1-benzhydryl-3,5-bis(4,5-dimethyl-1-imidazolylmethyl)-1,2,4-triazole (**6b**; 1.3 g, 2.8 mmol) in dry acetonitrile (300 mL) at 25 °C under nitrogen, and the mixture was then maintained in a bath at about 85 °C for 48 h. For compound **4a**·2 Cl, the resulting suspension was filtered, and the crude solid was identified. For compound **4b**·2 Cl, the solvent was removed in a rotary evaporator, and the solid residue was triturated with dry acetonitrile (5 × 10 mL) and filtered to afford macrocycle **4b**·2 Cl.

***N*-Benzhydryl macrocyclic dication 4a·2Cl**: (Scheme 2) A solution of 3,5-bis(chloromethyl)-1,2,4-triazole (**7**; 148 mg, 0.9 mmol) in dry acetonitrile (40 mL) was added dropwise to a stirred solution of 1-benzhydryl-3,5-bis(1-imidazolylmethyl)-1,2,4-triazole (**6a**; 356 mg, 0.9 mmol) in dry acetonitrile (350 mL) at 25 °C under nitrogen, and the mixture was then maintained in a bath at about 85 °C for 48 h. The resulting suspension was filtered, and the crude solid was identified as **4a**·2 Cl. The liquid filtrates were evaporated to dryness, and the residue was analyzed by ^{1}H NMR to assess the content of **4a**·2 Cl (Scheme 2). The total yield of the macrocycle was 60%. When the reaction was carried out under the same conditions in the presence of tetrabutylammonium chloride hydrate (1.35 g, 4.5 mmol) the total yield of macrocycle **4a**·2 Cl was 33%.

Betaines 5a·Cl and 5b·Cl: (Table 2) A solution of **4a**·2 Cl (56 mg, 0.1 mmol) in ethanol (90%, 20 mL) or **4b**·2 Cl (60 mg, 0.1 mmol) in ethanol (96%, 25 mL) was passed through a column packed with an Amberlite IRA-401 anion-exchange resin (hydroxide form). The neutral eluates were collected in a mixture of HCl (10%, 0.1 mmol) and ethanol (96%, 5 mL). The solution was evaporated to dryness to give the corresponding monochlorides **5a**·Cl and **5b**·Cl.

Betaine 5a·PF_6: (Table 2) A solution of macrocycle **4a**·2 Cl (56 mg, 0.1 mmol) in ethanol (90%, 20 mL) was passed through a column packed with strongly basic anion-exchange resin (Amberlite IRA-401, hydroxide form). The neutral eluates were acidified to pH 6 with hexafluorophosphoric acid, and the solution was evaporated to dryness to afford the hexafluorophosphate **5a**·PF_6.

Macrocycles 8a·2I and 9a·2I: (Table 2) *n*-Butyl iodide (0.34 mL, 3 mmol) was added to a suspension of the bis-betaine **1a** (97 mg, 0.3 mmol) in dry acetonitrile (75 mL) under nitrogen, and the mixture was heated under reflux for 48 h. After being cooled down to room temperature, the reaction mixture was filtered to recover 17 mg (18%) of the starting material **1a**. The liquid filtrates were evaporated to dryness, and the residue was triturated with dry diethyl ether (3 × 5 mL). The solid obtained was filtered and dried, to afford a mixture (87 mg, 42%) of *N*-alkylated isomers **8a**·2 I and **9a**·2 I in the proportion 60:40 as determined by ^{1}H NMR analysis of an aliquot of the mixture. A portion of the mixture (120 mg, 0.15 mmol) was triturated with hot dry acetone (3 × 10 mL). The white solid obtained was filtered and dried to give a mixture of isomers **8a**·2 I and **9a**·2 I (90:10). The liquid filtrates were evaporated to dryness to afford 36 mg (30%) of pure isomer **9a**·2 I.

Macrocycle 9a·2PF_6: (Table 2) A solution of macrocycle **9a**·2 I (11 mg, 0.014 mmol) in ethanol (90%, 20 mL) was passed through a column packed with a strongly basic anion-exchange resin (Ion exchanger III, Merck, hydroxide form). The neutral eluates were acidified to pH 3–4 with an aqueous solution of hexafluorophosphoric acid, and the solution was evaporated to dryness to afford the hexafluorophosphate **9a**·PF_6 (8 mg, 69%).

Macrocycles 8c·2I and 9c·2I: (Table 4) *n*-Butyl iodide (0.17 mL, 1.5 mmol) was added to a solution of the bis-betaine **1c** (164 mg, 0.3 mmol) in dry acetonitrile (75 mL) under nitrogen, and the mixture was heated under reflux for 4 h. After cooling down to room temperature, the solution was evaporated to dryness, and the residue was triturated with dry diethyl ether (3 × 5 mL). The solid obtained was filtered and dried to afford a mixture of *N*-alkylated isomers **8c**·2 I and **9c**·2 I (211 mg, 77%, 60:40) as determined by ^{1}H NMR analysis of an aliquot of the mixture. A portion of the mixture (50 mg, 0.05 mmol) was triturated with dry acetone (3 × 10 mL). The white solid obtained was filtered and dried to give a mixture of isomers **8c**·2I and **9c**·2I (90:10). The liquid filtrates were evaporated to dryness to afford 28 mg (55 %) of pure isomer **8c**·2I.

Alternatively, a solution of the mixture of isomers (103 mg, 0.11 mmol) in ethanol (96 %, 50 mL) was passed through a strongly basic anion-exchange resin (Ion exchanger III, Merck, hydroxide form). The eluates were collected by means of a 10 % hydrogen chloride solution in dry diethyl ether (pH 3–4). The resulting solution was evaporated to dryness to give a mixture of isomers **8c**·2Cl and **9c**·2Cl, which was chromatographed on alumina with a mixture of isopropanol/water (7:3) as the solvent system, to afford a sample of pure isomer **8c**·2Cl (7 mg, 9 %) and 68 mg (91 %) of a mixture of isomers **8c**·2Cl and **9c**·2Cl (95:5).

Macrocycles 11a·2Cl, 12a·2Cl: (Table 2) A solution of 1-benzhydryl-3,5-bis(chloromethyl)-1,2,4-triazole (**10**; 0.084 g, 0.25 mmol) in dry acetonitrile (20 mL) was added dropwise to a stirred solution of 1-benzhydryl-3,5-bis(1-imidazolylmethyl)-1,2,4-triazole (**6a**; 0.1 g, 0.25 mmol) in dry acetonitrile (90 mL) at 25 °C under nitrogen, and the mixture was then maintained at about 85 °C in a bath for 48 h. Analysis of an aliquot of the reaction mixture indicated the formation of a mixture of isomers **11a**·2Cl and **12a**·2Cl (1:1). The suspension was then filtered, and the crude white solid was identified as **11a**·2Cl (25 mg, 14 %). The liquid filtrates were evaporated to dryness to afford 78 mg (41 %) of a mixture of isomers **11a**·2Cl and **12a**·2Cl (1:2).

Single-crystal diffraction analysis of bis-betaine 1a and betaine 2a·PF$_6$:

*Bis-betaine **1a***: $C_{14}H_{14}N_{10}\cdot 4H_2O$, $M_w = 394.4$, $P2_1/n$, $a = 15.158(2)$, $b = 6.345(1)$, $c = 9.393(3)$ Å, $\beta = 99.65(2)^\circ$, $V = 890.7(1)$ Å^3, $Z = 2$, $F(000) = 416$, $\rho_{calcd} = 1.471$ g cm^{-3}, $\mu = 0.95$ cm^{-1}. Data were collected on a Siemens–Stoe AED diffractometer with $Cu_{K\alpha}$ radiation at room temperature, graphite monochromator and $\omega{:}\theta$ scan up to $2\theta = 120^\circ$ provided 1300 independent reflections, of which 1212 with $F_o > 4s(F_o)$ were used for refinements.

*Betaine **2a**·PF$_6$*: $C_{14}H_{15}N_{10}\cdot PF_6$, $M_w = 468.3$, $P2_1/c$, $a = 15.333(2)$, $b = 15.024(3)$, $c = 16.745(1)$ Å, $\beta = 106.59(1)^\circ$, $V = 3696.8(1)$ Å^3, $Z = 8$, $F(000) = 1904$, $\rho_{calcd} = 1.679$ g cm^{-3}, $\mu = 2.14$ cm^{-1}. Data collected as above yielded 5440 unique reflections, of which 3885 with $F_o > 4s(F_o)$ were used for refinement.

For both structures, the previously reported coordinates of the non-hydrogen atoms[4a] were used as a starting point for refinement by SHELXL97.[11a] Hydrogen atoms, including those of the solvent molecules for structure **1a**, were found by Fourier difference synthesis. Anisotropic thermal parameters were refined for all non-hydrogen atoms, and fixed coordinates and isotropic thermal parameters were used for hydrogen atoms. The final discrepancy indices are $R_1 = 0.037$ and $wR_2 = 0.104$ for structure **1a** and $R_1 = 0.054$ and $wR_2 = 0.466$ for **2a**·PF$_6$. Geometric calculations were performed with PARST.[11b] The molecular plots and packing diagrams were generated by PLATON.[11c] The hydrogen-bond networks were analyzed by means of the graph-set approach[11d] as implemented in the RPLUTO program.[11e,f]

Acknowledgement

This research was financially supported by the Dirección General de Investigación (MCYT, Spain) through project PB 98–1164. Additional support came from the Comissionat per a Universitats i Recerca de la Generalitat de Catalunya through grant 1999SGR-77. We give thanks to Dr. Irene Fernández and Dr. Marta Vilaseca, Servei de EM de la Divisió III–Universitat de Barcelona, for running ESI mass spectra. N.M. and S.R. thank the Universitat de Barcelona for fellowships.

---

[1] E. Alcalde, N. Mesquida, M. Gisbert, L. Pérez-García, *Eur. J. Org. Chem.* **2001**, in press.

[2] a) *Templated Organic Synthesis* (Eds.: F. Diederich, P. J. Stang), Wiley-VCH, Weinheim, **2000**; b) J. S. Bradshaw, R. M. Izatt, *Acc. Chem. Res.* **1997**, *30*, 338–345; c) *Comprehensive Supramolecular Chemistry, Vols. 1, 2* (Eds.: J. L. Atwood, J. E. D. Davies, D. D. Macnicol, F. Vögtle), Pergamon, Oxford, **1996**; d) J. W. Steed, J. L. Atwood, *Supramolecular Chemistry*, Wiley, Chichester, **2000**.

[3] a) V. Balzani, A. Credi, F. M. Raymo, J. F. Stoddart, *Angew. Chem.* **2000**, *112*, 3484–3530; *Angew. Chem. Int. Ed.* **2000**, *39*, 3348–3391; b) C. P. Collier, G. Mattersteig, E. W. Wong, Y. Luo, K. Beverly, J. Sampaio, F. M. Raymo, J. F. Stoddart, J. R. Heath, *Science* **2000**, *289*, 1172–1175.

[4] a) E. Alcalde, M. Alemany, L. Pérez-García, M. L. Rodriguez, *J. Chem. Soc. Chem. Commun.* **1995**, 1239–1240; b) E. Alcalde, M. Alemany, M. Gisbert, *Tetrahedron* **1996**, *52*, 15171–17188.

[5] a) E. Alcalde, L. Pérez-García, C. Miravitlles, J. Rius, E. Valentí, *J. Org. Chem.* **1992**, *57*, 4829–4834, and references therein; b) E. Alcalde, N. Mesquida, M. Vilaseca, *Rapid Commun. Mass Spectrom.* **2000**, *14*, 1443–1447.

[6] a) V. P. W. Böhm, W. A. Herrmann, *Angew. Chem.* **2000**, *112*, 4200–4202; *Angew. Chem. Int. Ed.* **2000**, *39*, 4036–4038; b) A. J. Arduengo, *Acc. Chem. Res.* **1999**, *32*, 913–921.

[7] J. S. Bradshaw, R. B. Nielsen, P.-K. Tse, G. Arena, B. E. Wilson, N. K. Dalley, J. D. Lamb, J. J. Christensen, R. M. Izatt, *J. Heterocyclic Chem.* **1986**, *23*, 361–368.

[8] E. Alcalde, S. Ramos, L. Pérez-García, *Org. Lett.* **1999**, *1*, 1035–1038.

[9] E. Alcalde, N. Mesquida, I. Fernández, E. Giralt, *Rapid Commun. Mass Spectrom.* **2000**, *14*, 1014–1016.

[10] E. Alcalde, M. Gisbert, C. Alvarez-Rúa, S. García-Granda, *Tetrahedron* **1996**, *52*, 15189–15196.

[11] a) G. M. Sheldrick, SHELXL97, University of Göttingen, Germany; b) M. Nardelli, PARST, University of Parma, Italy; c) A. L. Spek, PLATON, A multipurpose crystallographic tool, University of Utrecht, The Netherlands; d) J. Bernstein, R. E Davis, L. Shimoni, N.-L. Chang, *Angew. Chem.* **1995**, *107*, 1687–1706; *Angew. Chem. Int. Ed. Engl.* **1995**, *34*, 1555–1573; e) W. D. S. Motherwell, G. P. Shields, F. H. Allen, *Acta Crystallogr.* **1999**, *B55*, 1044–1056; f) W. D. S. Motherwell, G. P. Shields, F. H. Allen, *Acta Crystallogr.* **2000**, *B56*, 466–473.

[12] a) The crystalline and molecular structures for three examples of crown ethers containing 1*H*-1,2,4-triazole[7,12b] and a 1,2,4-triazolate moieties[12c] have been reported; b) J. S. Bradshaw, C. W. McDaniel, B. D. Skidmore, R. B. Nielsen, B. E. Wilson, N. K. Dalley, R. M. Izatt, *J. Heterocyclic Chem.* **1987**, *24*, 1085–1092; c) J. S. Bradshaw, D. A. Chamberlain, P. E. Harrison, B. E. Wilson, G. Arena, N. K. Dalley, J. D. Lamb, R. M. Izatt, *J. Org. Chem.* **1985**, *50*, 3065–3069.

[13] a) N. Mesquida, PhD thesis, Universitat de Barcelona (Spain), **1999**; b) S. Ramos, Masters Degree Dissertation, Universitat de Barcelona (Spain), **1998**.

Received: May 31, 2001 [F3307]